Threshold and Modal Characteristics of Composite-Resonator Vertical-Cavity Lasers

Daniel M. Grasso, *Student Member, IEEE,* and Kent D. Choquette, *Fellow, IEEE*

***Abstract*—We report the operation of a vertical-cavity surface-emitting laser (VCSEL) with two active, coupled optical cavities. In contrast to a conventional single-cavity VCSEL, the coupling between the two electrically independent active regions produces emission into two longitudinal modes. The light output versus current characteristics are presented under various biasing conditions in each cavity. Laser operation is achieved with current injection into only one cavity, and additional current injected into the other cavity changes the effective threshold current measured. The longitudinal and transverse modes are characterized, and it is found that the modal evolution of the laser can be modified by current injection into each cavity.**

***Index Terms*—Coupled cavity, modal evolution, threshold current, vertical-cavity surface-emitting laser (VCSEL).**

I. Introduction

VERTICAL-CAVITY surface-emitting lasers (VCSELs) have emerged as the dominant light source for short-distance optical communications. The advantages of VCSELs over conventional edge-emitting lasers include low threshold currents, lasing into a single longitudinal mode, and inherent high-speed operation [1]. For emerging optical networking applications, there is a need for control of the optical properties of the device. Previous research on edge-emitting semiconductor lasers has demonstrated additional functionality through the use of multiple sections, such as the cleaved-coupled-cavity (C^3) laser. The C^3 structure typically includes a passive secondary cavity that acts as a source of frequency-selective absorption. This technique has been used to obtain single longitudinal mode operation and wavelength tunability from a coupled cavity, where the single cavities alone would support multiple modes [2]–[4]. More recently, these ideas have been extended to vertical coupled cavity laser structures [5]–[14]. A VCSEL with two optically coupled cavities will be referred to as a *composite-resonator vertical-cavity laser* (CRVCL). The CRVCL has been used to obtain dual longitudinal wavelength operation [5], high single transverse mode power [7], Q-switched operation [8], picosecond pulse generation [9], and high-contrast optical switching [10].

In this paper, the threshold and modal characteristics are reported for a CRVCL with two active cavities. We show that the unique features of the laser output characteristics are determined and can be controlled by the details of the coupled cavity configuration. We find that, in contrast to a conventional VCSEL, the threshold current is a function of the current injected into each cavity. We show that, if current injection into one cavity brings the device to threshold, additional current injected into the other cavity causes a logarithmic decrease in the effective threshold current measured. In addition, the transverse and longitudinal mode characteristics are compared to a conventional, single-cavity VCSEL. It is shown that output characteristics can be controlled through selection of the current levels in the two cavities. The VCSEL structure and experimental setup are described in Section II. In Sections III and IV, the threshold and modal characteristics are examined, respectively. The paper concludes with potential applications and future work.

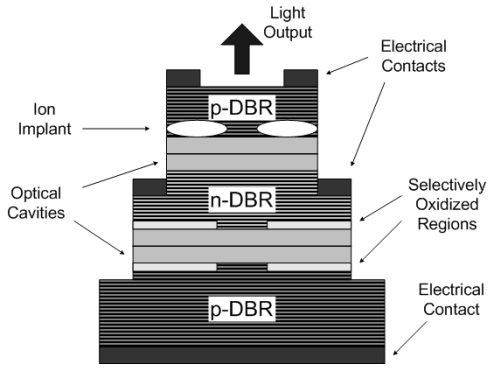

Fig. 1. Device structure of a CRVCL.

II. Device Structure and Experiment

The device characterized in this work is a CRVCL with two active cavities. A schematic is shown in Fig. 1. The CRVCL is grown by metalorganic vapor phase epitaxy and is composed of a monolithic bottom distributed Bragg reflector (DBR) with 35 periods, a middle DBR with 14.5 periods, and a top DBR with 21 periods. The mirror layers separate two 1-λ-thick optical cavities, each of which contain five GaAs quantum wells (QWs). The top cavity is defined using ion implantation, with an aperture of 6 μm. The bottom cavity has an aperture of approximately 10 μm and is defined using selective oxidation [1]. The device is fabricated in a double-mesa structure to allow for independent electrical injection into either cavity. The light output versus current (L–I) characteristics were measured by on-wafer probing with a semiconductor parameter analyzer and a Si photodetector. The second cavity was simultaneously biased with a precision power supply. The transverse mode measurements were taken with an optical spectrum analyzer and each cavity was biased with a separate precision power supply.

Manuscript received April 11, 2003; revised September 12, 2003. This work was supported by the National Science Foundation under Grant 0121662.

The authors are with the Department of Electrical and Computer Engineering, University of Illinois at Urbana-Champaign, Urbana, IL 61801 USA.

Digital Object Identifier 10.1109/JQE.2003.819544

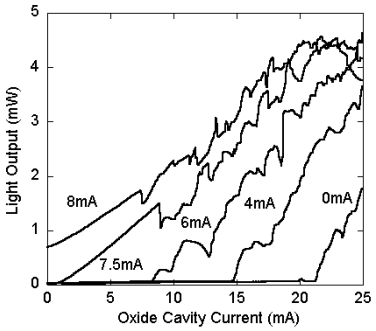

Fig. 2. Output characteristics for varying current into oxide-confined cavity. Ion-implanted cavity currents are labeled.

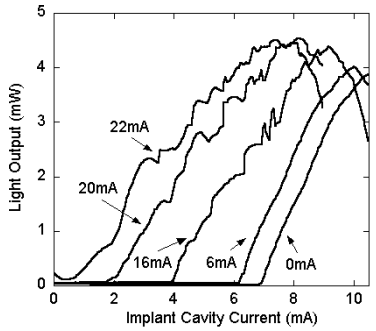

Fig. 3. Output characteristics for varying current into ion-implanted cavity. Oxide-confined cavity currents are labeled.

III. Threshold Conditions

A. Absorption Properties of the Secondary Cavity

The additional optical cavity of the CRVCL device admits new functionality since two injection currents can be varied independently. Figs. 2 and 3 show the *L–I* characteristics of the CRVCL obtained while varying the current into one cavity with a fixed current into the other cavity [14]. For example, Fig. 2 corresponds to varying the drive current into the bottom oxide-confined cavity with various fixed injection currents into the top ion-implanted cavity. The cavity with variable current will be referred to as the *primary cavity*, and the cavity with constant current will be referred to as the *secondary cavity*. The output characteristics shown in Figs. 2 and 3 are similar to that of a single cavity VCSEL. The variations of the output light with increasing current indicate a rich transverse mode spectrum, as described in Section IV. A unique feature of the *L–I* characteristics observed in Figs. 2 and 3 is the decrease in primary cavity threshold current measured with increasing current in the secondary cavity. With sufficient injection current in the secondary cavity, the threshold current measured in the primary cavity is reduced to zero. We define the effective threshold current to be the value measured in the primary cavity. For example, in Fig. 3, the effective threshold current is 4 mA when the secondary cavity current is 16 mA. In contrast to Figs. 2 and 3, output characteristics reported in [6] for a passive/active CRVCL structure showed no change in the threshold current with current injection into the secondary cavity.

The large threshold current values obtained with no injection into the secondary cavity (open circuit) suggests variable QW absorption as a mechanism for the change in threshold current. Similar to the use of a Fabry–Perót etalon in a C^3 laser [2], we assume that the second cavity is a source of variable absorption for the coupled structure. When the secondary cavity has no electric potential applied, the QWs strongly absorb light, with a typical value of absorption coefficient of $\alpha \approx 10^4$ cm^{-1} per well [15]. Although the QW layers are thin, most VCSEL structures are designed so that the optical field antinode overlaps the QWs [1]. This implies that an optical field induced from gain of the primary cavity will also be strongly attenuated by the secondary cavity. Because of this loss, we find that the threshold currents measured with the secondary cavity open circuited are relatively high. In fact, only some of the devices tested were found to lase with current injection into only one cavity. As current is injected into the QWs of the secondary cavity, the absorption is reduced until transparency. If additional current is added, the secondary cavity will also provide gain. This implies that the effective threshold current will depend on the secondary cavity current.

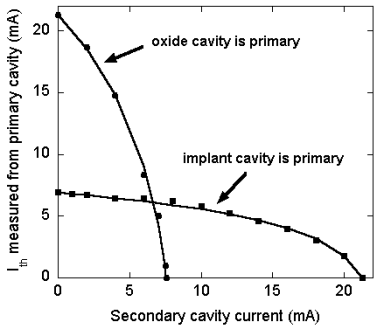

Fig. 4. Comparison of effective threshold current measured in the primary cavity for different current injection conditions in the secondary cavity.

B. Effective Threshold Current

Fig. 4 (solid points) is a plot of the effective threshold current versus the current injected into the secondary cavity. The figure includes two configurations: one where the oxide cavity is the primary cavity and the implant cavity is the secondary cavity, and vice versa. The solid line through each data set is a curve fit that determines the effective threshold current, $I_{\rm th}$, as a function of the secondary cavity current $I_{\rm sc}$. We use the equation

$$I_{\rm th}(I_{\rm sc}) = A\ln(B - cI_{\rm sc}). \tag{1}$$

The parameters B and c are determined from the conditions $I_{\rm th} = 0$ and $I_{\rm sc} = 0$. The value of A is chosen to minimize the mean-square error between (1) and the measured data. As shown in Table I, the values of A for the two biasing schemes are different. If the CRVCL had identical transverse optical confinement in each cavity, the two data sets in Fig. 3 would be expected to overlap and intersect each axis at the same current value. However, significant asymmetry results from the different confinement mechanisms (ion-implanted versus oxide-confined) and aperture size of the cavities (see Fig. 1). The trend of decreasing effective threshold current with increasing current in the secondary cavity agrees with the qualitative analysis given in Section III-A.

TABLE I
PARAMETERS USED IN THRESHOLD CURRENT DATA

	Implant Cavity Primary	Oxide Cavity Primary
A	10.44	2.29
B	7.68	20.6
c $(mA)^{-1}$	0.88	0.92

IV. OPTICAL MODES

The additional optical cavity and middle mirror of the CRVCL impact the spectral properties of the device. Although the two cavities are composed of the same material and containing the same number of QWs, the optically coupled structure causes a wavelength splitting between the two degenerate longitudinal modes.

A. Theoretical Modeling of Transverse Modes

The transverse mode splitting in VCSEL structures is analyzed following [16]. It is assumed that the VCSEL geometry and the cavity effective refractive index profile both have cylindrical symmetry. It is assumed in this model that the refractive index profile is the truncated parabola

$$n^2(r) = \begin{cases} n_c^2\left(1 - \frac{2\Delta r^2}{a^2}\right), & r \le a \\ n_s^2, & r > a \end{cases} \quad (2)$$

where

$$\Delta = \frac{n_c^2 - n_s^2}{2n_c^2} \approx \frac{n_c - n_s}{n_c}. \quad (3)$$

Here, n_c and n_s are the refractive indices of the optical cavity and the surroundings, respectively, in analogy to "core" and "cladding" of an optical fiber. For an ion-implanted device, the n_c value refers to the region where the thermal lens is formed. For an oxide-confined device, n_s is the refractive index of the oxide layer. The approximation in (3) holds when $n_c - n_s \ll n_c$, which is always satisfied. The solutions to the Helmholtz equation allow determination of the transverse mode spacing

$$\Delta\lambda = |\lambda_{lm} - \lambda_{pq}| = |2(m-q) + l - p| \frac{\sqrt{n_c - n_s}}{\sqrt{2}\pi n_c^{3/2}} \frac{\lambda^2}{a} \quad (4)$$

where l, m, p, and q are integers identifying a particular transverse mode. An important result of this formalism is that the wavelength spacing between any two adjacent modes is constant. Shown in Table II are the numerical values used for each parameter, and the resulting calculated transverse mode spacing $\Delta\lambda$ between the first two transverse modes for the device under study.

B. Experimental Results

In this section, the measured spectral characteristics are presented under various current injection conditions. Shown in Fig. 5 is the modal evolution of the device when the oxide-confined cavity is open circuited, and current is injected only into the ion-implanted cavity. Since all of the current is injected into the implanted cavity, the modal evolution with current should appear similar to that of a single-cavity ion-implanted VCSEL. However, there is the possibility of lasing in two longitudinal modes, each with a family of transverse modes. As seen in Fig. 5, the fundamental mode begins to lase first, and the device remains single mode near threshold. This is similar to the behavior of a single-cavity ion-implanted VCSEL [1]. As the current is increased, higher order modes begin to lase at progressively shorter wavelengths. Additionally, the output wavelength of each mode shifts to longer wavelengths. This is due to parasitic resistive heating, which has similar effects on the modal properties of conventional VCSELs. In Fig. 5, only one longitudinal mode is present. The transverse mode spacing remains fairly constant between adjacent modes, as predicted by (4).

TABLE II
NUMERICAL VALUES FOR TRANSVERSE MODE SPACING MODEL

Model Parameter	Value (Implant Cavity)	Value (Oxide Cavity)
$n_c - n_s$	0.006	0.0122
λ_B (nm)	850	850
a (μm)	3	5
calculated $\Delta\lambda$ (nm)	0.73	0.59
measured $\Delta\lambda$ (nm)	0.86	0.45

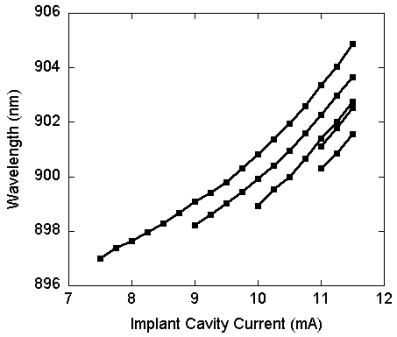

Fig. 5. Modal evolution with varying current injection only into the ion-implanted cavity.

Shown in Fig. 6 is the modal evolution of the device when the ion-implanted cavity is open circuited, and current is injected only into the oxide-confined cavity. Comparisons can again be drawn to the spectral characteristics of a single-cavity, oxide-confined VCSEL [18]. Fig. 6 shows emission at multiple transverse modes, even near threshold. As the current is increased, higher order modes begin to lase and the emission shifts to longer wavelengths. In contrast to Fig. 5, the family of transverse modes for each longitudinal mode can be seen from threshold. Since the shorter wavelength set of transverse modes (around 891 nm) are apparent at threshold in Fig. 6 but not in Fig. 5, this may indicate that the shorter longitudinal mode is located predominantly in the lower oxide-confined cavity. Although the QWs and the longitudinal cavity lengths are identical, the different transverse confinement will influence the relative distribution of each mode between the top and bottom cav-

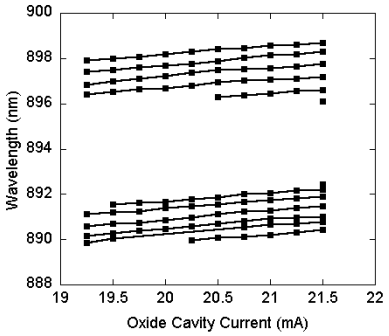

Fig. 6. Modal evolution with varying current injection only into oxide-confined cavity.

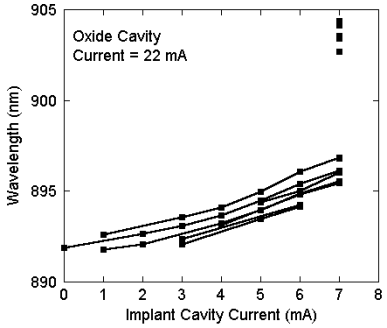

Fig. 7. Modal evolution with varying current injection into ion-implanted cavity and 22 mA injected into bottom oxide-confined cavity.

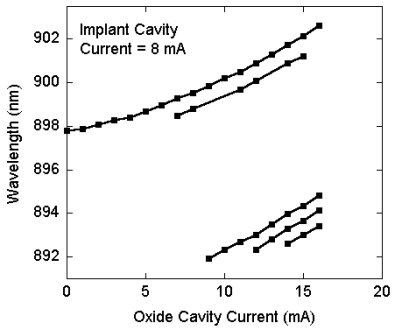

Fig. 8. Modal evolution with varying current injection into bottom oxide-confined cavity and 8 mA injected into ion-implanted cavity.

ities. As intermediate cases, Figs. 7 and 8 show the modal evolution with current injected into both cavities. In these two figures, the current injected into the secondary cavity is sufficient to produce a zero effective threshold current in the primary cavity. The output for each case is single mode at threshold. However, the fundamental transverse mode lases first in Fig. 8 but not Fig. 7. Both longitudinal modes eventually begin to lase in these figures, although again the longitudinal mode with longer wavelength does not necessarily begin to lase at threshold. In general, the characteristics of Figs. 7 and 8 are a combination of the behaviors exhibited in the ion-implanted cavity case of Fig. 5 and the oxide-confined cavity case of Fig. 6.

In Table II, the calculated and measured transverse mode spacing, measured between the fundamental and first higher order transverse mode that begins to lase, are compared. In each case the measurement is taken under current injection into only one cavity, the second cavity remaining open circuited, and an effective mirror length of 4 μm is used. Both calculated transverse mode spacings compare well with the measured values.

V. Conclusion

In this work, the CW operation of a coupled-cavity VCSEL is reported. The CRVCL has two optically coupled but electrically independent cavities with asymmetric transverse confinement. It is shown that the output characteristics are a function of the current injected into each of the cavities. The threshold condition is found to depend on the currents injected into both cavities. The output characteristics presented show that it is possible to obtain lasing with a threshold current that is apparently zero through the use of a secondary cavity current. In addition, the modal evolution is also presented under various biasing conditions in each cavity. The calculated transverse mode spacing is compared with the spacing from the eigenfunctions of a conventional, single-cavity VCSEL. The output wavelength can be tuned by selection of the two cavity currents, which determines lasing of one (or both) of the two longitudinal modes.

Much of the asymmetry observed in the output and spectral characteristics is a consequence of differences in the aperture size and confinement mechanisms of the two cavities. A device with two or more cavities having a low threshold current and multiple longitudinal modes could have applications for coarse wavelength division multiplexing networks. By exploiting the effective threshold current in the CRVCL, high efficiency modulation could be designed for data communication applications.

Acknowledgment

The authors thank A. Allerman, W. Chow, A. Fischer, K. Geib, and D. Serkland at Sandia National Laboratories. The authors also thank the reviewers for their comments.

References

[1] K. D. Choquette and K. M. Geib, "Fabrication and performance of vertical-cavity surface-emitting lasers," in *Vertical-Cavity Surface-Emitting Lasers*, C. Wilmsen, H. Temkin, and L. Coldren, Eds. New York: Cambridge Univ. Press, 1999, pp. 193–232.

[2] W. T. Tsang, "The cleaved-couple-cavity laser," in *Semiconductors and Semimetals*. Orlando, FL: Academic, 1985, pt. B, vol. 22, pp. 257–373.

[3] Y. Suematsu, M. Yamada, and K. Hayashi, "Integrated twin-guide AlGaAs laser with multiheterostructure," *IEEE J. Quantum Electron.*, vol. QE-11, pp. 457–460, 1975.

[4] L. A. Coldren, B. I. Miller, K. Iga, and J. A. Rentchler, "Monolithic two-section GaInAsP/InP active-optical-resonator devices formed by reactive ion etching," *Appl. Phys. Lett.*, vol. 38, pp. 315–317, 1981.

[5] R. P. Stanley, R. Houdre, U. Oesterle, M. Ilegems, and C. Weisbuch, "Coupled semiconductor microcavities," *Appl. Phys. Lett.*, vol. 65, no. 16, pp. 2093–2095, 1994.

[6] A. J. Fischer, K. D. Choquette, W. W. Chow, H. Q. Hou, and K. M. Geib, "Coupled-resonator vertical-cavity laser diode," *Appl. Phys. Lett.*, vol. 75, no. 19, pp. 3020–3022, 1999.

[7] A. J. Fischer, K. D. Choquette, W. W. Chow, A. A. Allerman, D. K. Serkland, and K. M. Geib, "High single-mode power observed from a coupled-resonator vertical-cavity laser diode," *Appl. Phys. Lett.*, vol. 79, no. 25, pp. 4079–4081, 2001.

[8] A. J. Fischer, K. D. Choquette, W. W. Chow, A. A. Allerman, and K. M. Geib, "Q-switched operation of coupled-resonator vertical-cavity laser diode," *Appl. Phys. Lett.*, vol. 76, no. 15, pp. 1975–1977, 2000.

[9] P. Michler, M. Hilpert, and G. Reiner, "Dynamics of dual-wavelength emission from a coupled semiconductor microcavity laser," *Appl. Phys. Lett.*, vol. 70, no. 16, pp. 2073–2075, 1997.

[10] A. J. Fischer, K. D. Choquette, W. W. Chow, A. A. Allerman, and K. M. Geib, "Bistable output from a coupled-resonator vertical-cavity laser diode," *Appl. Phys. Lett.*, vol. 77, no. 21, pp. 3319–3321, 2000.

[11] M. Brunner, K. Gulden, M. Moser, J. F. Carlin, R. P. Stanley, and M. Ilegems, "Continuous-wave dual-wavelength lasing in a two-section vertical cavity laser," *IEEE Photon. Technol. Lett.*, vol. 12, pp. 1316–1318, Oct. 2000.

[12] J. F. Carlin, R. P. Stanley, P. Pellandini, U. Oesterle, and M. Ilegems, "The dual wavelength bi-vertical cavity surface-emitting laser," *Appl. Phys. Lett.*, vol. 75, no. 7, pp. 908–910, 1999.

[13] P. Pellandini, R. P. Stanley, R. Houdre, U. Oesterle, M. Ilegems, and C. Weisbuch, "Dual wavelength laser emission from a coupled semiconductor microcavity," *Appl. Phys. Lett.*, vol. 71, no. 7, pp. 864–866, 1997.

[14] D. M. Grasso, K. D. Choquette, D. T. Mathes, R. Hull, A. J. Fischer, W. W. Chow, K. M. Geib, and A. A. Allerman, "Threshold characteristics of composite resonator vertical cavity lasers," in *Proc. Conf. Lasers and Electro-Optics 2002*, 2002, p. 468.

[15] L. A. Coldren and S. W. Corzine, *Diode Lasers and Photonic Integrated Circuits*. New York: Wiley, 1995.

[16] K. J. Ebeling, "Analysis of vertical cavity surface emitting laser diodes," in *Proc. 50th Scottish Universities Summer School in Physics*, Philadelphia, PA, 1999, pp. 295–338.

[17] C. J. Chang-Hasnain, M. Orenstein, A. Von Lehmen, L. T. Florez, J. P. Harbison, and N. G. Stoffel, "Transverse mode characteristics of vertical cavity surface-emitting lasers," *Appl. Phys. Lett.*, vol. 57, no. 3, pp. 218–220, 1990.

[18] S. P. Hegarty, G. Huyet, P. Porta, J. G. McInerney, K. D. Choquette, K. M. Geib, and H. Q. Hou, "Transverse-mode structure and pattern formation in oxide-confined vertical-cavity semiconductor lasers," *J. Opt. Soc. Amer. B*, vol. 16, pp. 2060–2071, 1999.

Daniel M. Grasso (S'03) received B.S. degrees in electrical engineering and mathematics from the State University of New York at Buffalo in 2000 and the M.S. degree in electrical engineering from the University of Illinois at Urbana-Champaign in 2002. He is currently working toward the Ph.D. in electrical engineering at the University of Illinois under Prof. Kent Choquette.

His research interests include fabrication and high-speed characterization of VCSELs and opto-electronic devices.

Kent D. Choquette (M'97–F'03) received B.S. degrees in engineering physics and applied mathematics from the University of Colorado-Boulder in 1984 and the M.S. and Ph.D. degrees in materials science from the University of Wisconsin-Madison in 1985 and 1990, respectively.

In 1990 he held a post-doctoral appointment at AT&T Bell Laboratories, Murray Hill, NJ, and in 1993 he joined Sandia National Laboratories, Albuquerque, NM. He became a Professor in the Electrical and Computer Engineering Department, University of Illinois at Urbana-Champaign, in 2000. His research group is centered around the design, fabrication, and characterization of vertical-cavity surface-emitting lasers (VCSELs), photonic crystals, and other optoelectronic devices. His research interests include new microcavity light sources, nanofabrication technologies, and hybrid integration techniques. He has authored over 100 publications and three book chapters and has presented numerous invited talks and tutorials on VCSELs.

Prof. Choquette is an Associate Editor of the IEEE JOURNAL OF QUANTUM ELECTRONICS, a Fellow of the IEEE Lasers and Electro-Optics Society (LEOS), and a member of the Optical Society of America (OSA). From 2000 to 2002 he was an IEEE/LEOS Distinguished Lecturer.